FERMILAB-PUB-13-021-AE-CD

A Catalog of Distance Determinations for the SEGUE K giants in the Galactic Halo

Xiang-Xiang Xue[1,2], Zhibo Ma[3], Hans-Walter Rix[1], Heather L. Morrison[3], Paul Harding[3], Timothy C. Beers[4],Inese I. Ivans[5], Heather R. Jacobson[6,7], Jennifer Johnson[8], Young Sun Lee[9,10], Sara Lucatello[11], Constance M. Rockosi[12], Jennifer S. Sobeck[13], Brian Yanny[14], Gang Zhao[2]

ABSTRACT

We present an online catalog of distance determinations for 4781 K giants, most of which are members of the Milky Way's stellar halo. Their spectra from SDSS/SEGUE provide metallicities with accuracies Δ[Fe/H] $\approx \pm 0.2$ dex and

[1]Max-Planck-Institute for Astronomy Königstuhl 17, D-69117, Heidelberg, Germany

[2]Key Lab of Optical Astronomy, National Astronomical Observatories, CAS, 20A Datun Road, Chaoyang District, 100012, Beijing, China

[3]Department of Astronomy, Case Western Reserve University, Cleveland, OH 44106, USA

[4]NOAO, Tucson, Arizona, 85719, USA

[5]Department of Physics and Astronomy, JFB#201, The University of Utah, Salt Lake City, 84112, USA

[6]Department of Physics & Astronomy, Michigan State University, East Lansing, MI 48823, USA

[7]Massachusetts Institute of Technology, Kavli Institute for Astrophysics and Space Research, 77 Massachusetts Avenue, Cambridge, MA 02139, USA

[8]Department of Astronomy, 4055 McPherson Laboratory, 140 W. 18th Ave, Columbus, Ohio, 43210, USA and Center for Cosmology and Astro-Particle Physics, 191 West Woodruff Ave, Columbus, Ohio 43210, USA

[9]Department of Astronomy, New Mexico State University, Las Cruces, NM 88003

[10]Department of Physics and Astronomy and JINA: Joint Institute for Nuclear Astrophysics, Michigan State University, E. Lansing, MI 48824, USA

[11]Osservatorio Astronomico di Padova, Vicolo dellOsservatorio 5, 35122 Padua, Italy

[12]Lick Observatory/University of California, Santa Cruz, CA 95060, USA

[13]Laboratoire Lagrange (UMR7293), Universite de Nice Sophia Antipolis, CNRS, Observatoire de la Cote dAzur, BP 4229, F-06304 Nice Cedex 04, France; JINA: Joint Institute for Nuclear Astrophysics and the Department of Astronomy and Astrophysics, University of Chicago, 5640 South Ellis Avenue, Chicago, IL 60637, USA

[14]Fermi National Accelerator Laboratory, P.O. Box 500, Batavia, IL 60510 USA

Operated by Fermi Research Alliance, LLC under Contract No. De-AC02-07CH11359 with the United States Department of Energy.

giant-dwarf distinction. The distance moduli are derived from a comparison of each star's apparent magnitude with the absolute magnitude of empirically calibrated color-luminosity fiducials, at the observed $(g-r)_0$ color and spectroscopic [Fe/H]. We employ a probabilistic approach that makes it straightforward to propagate the errors in metallicities, magnitudes, and colors properly into distance uncertainties. We also fold in *prior* information about the giant-branch luminosity function and different metallicity distributions of the SEGUE K-giant targeting sub-categories. We show that the metallicity prior plays little role in the distance estimates, but that neglecting the luminosity prior would lead to a systematic distance modulus bias of up to 0.2 mag. We find a median distance precision of 12%, with distance estimates most precise for the least metal-poor stars near the tip of the red-giant branch. We use globular and open clusters to verify the precision and accuracy of our distance estimates. The stars in our publicly available catalog are up to 110 kpc distant from the Galactic center, with 270 stars beyond 50 kpc, forming the largest sample of distant tracers in the Galactic halo.

Subject headings: galaxies: individual(Milky Way) – Galaxy: halo – stars: K giants – stars: distance

1. Introduction

K giants have long been used to map the Milky Way's stellar halo (Bond 1980; Ratnatunga & Bahcall 1985; Morrison et al. 1990, 2000; Starkenburg et al. 2009). In contrast to blue horizontal-branch (BHB) and RR Lyrae stars, giant stars are found in predictable numbers in old populations of all metallicities, and at the low metallicities expected for the MW halo they are predominantly K giants. At the same time, their high luminosities ($M_r \sim 1$ to -3) make it feasible to study them with current wide-field spectroscopic surveys to distances of > 100 kpc (Battaglia 2007). The Sloan Extension for Galactic Understanding and Exploration (Yanny et al. 2009, SEGUE), which has entered the second stage (SEGUE-2, Rockosi et al. *in preparation*), specifically targeted K giants for spectroscopy. For simplicity, henceforth we refer to SEGUE and SEGUE-2 collectively as simply SEGUE. The SEGUE data products include sky positions, radial velocities, apparent magnitudes, and atmospheric parameters (metallicities, effective temperatures, and surface gravities), but no distances.

Distance estimates to kinematic tracers, such as the K giants, are indispensable for studies of Milky Way halo dynamics - such as estimates of the halo mass (Battaglia et al. 2005; Xue et al. 2008), for exploring the formation of our Milky Way (e.g., probing velocity-position

correlations, Starkenburg et al. 2009; Xue et al. 2011), and for deriving the metallicity profile of the Milky Way stellar halo. All of these studies require not only unbiased distance estimates, but also a good understanding of the distance errors. However, unlike 'standard candles' (i.e., BHB and RR Lyrae stars), the (intrinsic) luminosities of K giants vary by two orders of magnitude, with color and luminosity depending on stellar age and metallicity. Furthermore, the lower (less luminous) part of the giant branch is 'steep' in the color-magnitude diagram (CMD), particularly for stars of low metallicity. For this reason, it turns out to be more difficult to obtain precise distances for K giants than for, say, main-sequence stars.

The most immediate approach for estimating a distance to a K giant with color c and metallicity [Fe/H] (e.g., from SDSS/SEGUE) is to simply look up its expected absolute magnitude M in a set of observed cluster fiducials, $\mathrm{M}\big(c, [\mathrm{Fe/H}]\big)$. Comparison with the apparent magnitude then yields the distance modulus (denoted by $\mathcal{DM}$) and distance. In practice, this simple approach has two problems. First, care is required to propagate the errors in metallicities, magnitudes, and colors properly into distance uncertainties. Secondly, such an approach does not immediately incorporate external prior information, such as the luminosity function along the red giant-branch (RGB) and the overall metallicity distribution of the stellar giant population under consideration. Because the luminosity function along the RGB is steep, and there are many more lower luminosity stars than high luminosity stars ($\mathrm{n}\big(\mathrm{L}\big) \sim \mathrm{L}^{-1.8}$; Sandquist et al. 1996, 1999), an estimate of the absolute magnitude, $\mathrm{M}(c, [\mathrm{Fe/H}])$, is more likely to produce an overestimate of the luminosity, and therefore an overestimate of the distance. Analogously, there are few extremely metal-poor or metal-rich stars observed in the halo; hence, a very low estimate of [Fe/H] is more likely an underestimate of the metallicity of an (intrinsically) less metal-poor star, and so the estimate of the absolute magnitude will lead to an overestimate the luminosity, and therefore an overestimate of the distance. Thus, to exploit K giants such as those from SDSS/SEGUE for various dynamical analyses, an optimal way to determine an unbiased distance probability distribution for each sample star is crucial.

A general probabilistic framework to make inferences about parameters of interest (e.g., distance moduli) in light of direct observational data and broader prior information is well-established. It has been applied in a wide variety of circumstances and recently also applied to the distance determinations for stars, including giant stars in the RAVE survey (Burnett & Binney 2010; Burnett et al. 2011). Burnett & Binney (2010) described how probability distributions for all the 'intrinsic' parameters (e.g., true initial metallicity, age, initial mass, distance, and sky position) can be inferred according to Bayes' theorem, drawing on the star's observables and the errors thereon. Here we focus on a somewhat more restricted problem: the distances to stars on the RGB, which we can presume to be 'old' (> 5 Gyr). Like any Bayesian approach, our approach is optimal in the sense that it aims

to account for all pertinent information, can straightforwardly propagate the errors of the observables to distance uncertainties, and should avoid systematic biases in distance estimates. This approach also provides a natural framework to account for the fact that distance estimates will be less precise for stars that fall onto a 'steep' part of the color-magnitude fiducial, presumably metal-poor stars on the lower portion of the RGB.

The goal of this paper is to outline and implement such a Bayesian approach for estimating the best and unbiased probability distribution of the distance moduli $\mathcal{DM}$, for each star in a sample of 4781 K giants from SDSS/SEGUE. This distribution can then be characterized by the most probable distance modulus, $\mathcal{DM}_{\rm peak}$, and the central 68% interval, $\Delta\mathcal{DM}$. At the same time, this approach of course also yields estimates for the absolute magnitude M, heliocentric distance d, Galactocentric distance $\rm r_{GC}$, and their corresponding errors.

In the next section, we introduce the selection of the SEGUE K giants and their observable properties. In §3, we describe a straightforward (Bayesian) method to determine the distances. The results and tests are presented in §4. Finally, §5 presents our conclusions and a summary of the results.

2. Data

SDSS and its extensions use a dedicated 2.5m telescope (Gunn et al. 2006) to obtain *ugriz* imaging (Fukugita et al. 1996; Gunn et al. 1998; York et al. 2000; Stoughton et al. 2002; Pier et al. 2003; Eisenstein et al. 2011, Smee, S. A., et al. 2012, AJ, submitted) and resolution (defined as $\rm R = \lambda/\Delta\lambda$) ∼1800 spectra for 640 objects in a 7 sq deg field simultaneously. SEGUE (Sloan Extension for Galactic Understanding and Exploration), one of the key projects of SDSS-II and SDSS-III, obtained some 360,000 spectra of stars in the Galaxy, selected to explore the nature of stellar populations from 0.5 kpc to 100 kpc (Yanny et al. 2009, and Rockosi et al *in preparation*). Data from SEGUE is a significant part of the ninth public data release, DR9 (Ahn, C., et al. 2012, ApJS, submitted).

SDSS DR9 delivers estimates of $\rm T_{eff}$, log g, and [Fe/H] from an updated and improved version of the SEGUE Stellar Parameter Pipeline (SSPP, Lee et al. 2008a,b; Allende Prieto et al. 2008; Smolinski et al. 2011). The SSPP processes the wavelength- and flux-calibrated spectra generated by the standard SDSS spectroscopic reduction pipeline (Stoughton et al. 2002), obtains equivalent widths and/or line indices for more than 80 atomic or molecular absorption lines, and estimates $\rm T_{eff}$, log g, and [Fe/H] through the application of a number of complementary approaches (see Lee et al. 2008a, for detailed description of these techniques

and Rockosi et al. *in preparation* for the changes and improvements of the SSPP).

Targeting K giants has been an important part of SEGUE's scientific aims, particularly in SEGUE-2. Because of the intrinsically low fraction of K giants in the Galaxy, SEGUE adopted sophisticated criteria mainly based on *ugriz* photometry and proper motions to preselect likely K-giant candidates for fiber-fed spectroscopic observation.

SEGUE targets K-giant candidates with $(g-r)_0$ between 0.5 and 1.3, $(u-g)_0$ between 0.5 and 3.5 (see Figure 1), and proper motions smaller than 11 mas/year. The K giants are designed to be selected in three sub-categories, named l-color[1] K giants, red K giants, and proper motion K giants. However, besides the three sub-categories, about 20% of our giant sample comes from stars which do not pass the target criteria described above (hereafter we referred to as serendipitous K giants.). The majority of serendipitous K giants were originally targeted as K giants, but as photometric reductions have improved, their *ugr* colors changed so that they are no longer in the target region. There are also a number of serendipitous K giants from different target-selection classes such as low-metallicity stars (which use a stronger cut on l color and no proper motion criteria) and G and K dwarfs (designed to study the disk, with only a simple cut in $g-r$). Figure 10 of Yanny et al. (2009) shows the regions of the $u-g/g-r$ plane occupied by K giants: each target category focuses on a particular region. The l-color K-giant category uses the metallicity sensitivity of the $u-g$ color for the bluer part of our color range to select metal-poor K giants. The other two categories focus on the redder stars with $(g-r)_0 > 0.8$. The red K-giant category selects those stars whose luminosity leads them to fall above the locus of foreground stars, while the proper motion K-giant region is where the K giants are found in the locus of foreground stars. Here only a proper motion selection can be used to cull out the nearby dwarf stars with appreciable proper motion. We further limit the sample by requiring that the reddening estimate from Schlegel et al. (1998) for each star E(B-V) is less than 0.25 mag.

In addition to the log g estimate provided by the pipeline, we employ a spectroscopic index in the region of the Mgb/MgH features, similar to that of Morrison et al. (2003), which is a strong indicator of luminosity. The SSPP continuum corrects the spectra using a polynomial, and this process can remove much of the strong MgH feature seen in dwarfs; thus we work with flux-corrected but not continuum-corrected data. We calibrate this index using spectra taken of globular and open cluster giants. This is described in full in Ma et al. (in preparation).

Using colors, reddening, [Fe/H], and log g values from DR9, we find 14,025 field candi-

[1] $\mathrm{l-color} = -0.436\mathrm{u} + 1.129\mathrm{g} - 0.119\mathrm{r} - 0.574\mathrm{i} + 0.1984$ and is a photometry metallicity indicator for stars in the color range $0.5 < (g-r) < 0.8$. Reference: Lenz et al. (1998).

dates which satisfy our K-giant criteria and have good photometry (i.e., color errors are less than 0.04 mag). We describe a further culling of the sample in §3.4, where we also describe the fiducials used to obtain distances to eliminate stars that could either be on the RGB or in the red clump. The sample has a typical color error of ±0.02 mag, a typical [Fe/H] error of ±0.2 dex, and a typical log g error of ±0.5 dex. The error of [Fe/H] for each K giant used in this paper is calibrated using cluster data plus repeat observations, which depends on the signal-to-noise ratio of the spectrum, as described in detail in Ma et al. (*in preparation*).

3. Probabilistic Framework for Distance Estimates

Our goal is to obtain the *posterior probability distribution* (pdf) for the distance modulus of any particular K-giant star, after accounting for (i.e., marginalizing over) the observational uncertainties in apparent magnitudes, colors, and metallicities (m, c, [Fe/H], Δm, Δc, Δ[Fe/H]), and after including available prior information about the K-giant luminosity function, metallicity distribution, and, possibly, the radial halo-density profile.

3.1. Distance Modulus Likelihoods

We start by recalling Bayes theorem, cast in terms of the situation at hand:

$$\mathrm{P}\big(\mathcal{DM} \mid \{m, c, [\mathrm{Fe/H}]\}\big) = \frac{\mathrm{P}\big(\{m, c, [\mathrm{Fe/H}]\} \mid \mathcal{DM}\big)\mathrm{p}_{\mathrm{prior}}\big(\mathcal{DM}\big)}{\mathrm{P}\big(\{m, c, [\mathrm{Fe/H}]\}\big)}. \tag{1}$$

Here, $\mathrm{P}\big(\mathcal{DM} \mid \{m, c, [\mathrm{Fe/H}]\}\big)$ is the pdf of the distance moduli ($\mathcal{DM} = \mathrm{m} - \mathrm{M}$), and describes the relative probability of different $\mathcal{DM}$, in light of the data, $\{m, c, [\mathrm{Fe/H}]\}$ (we use $\{$ $\}$ to denote the observational constraints, i.e., the estimates and the uncertainties for the observable quantities). $\mathrm{P}\big(\{m, c, [\mathrm{Fe/H}]\} \mid \mathcal{DM}\big)$ is the *likelihood* of $\mathcal{DM}$ (e.g., $\mathscr{L}\big(\mathcal{DM}\big)$), and tells us how probable the data $\{m, c, [\mathrm{Fe/H}]\}$ are if $\mathcal{DM}$ were true. The term $\mathrm{p}_{\mathrm{prior}}\big(\mathcal{DM}\big)$ is the *prior probability* for the $\mathcal{DM}$, which reflects independent information about this quantity, e.g., that the stellar number density in the Galactic halo follows a power law of r^{-3}. The term $\mathrm{P}\big(\{m, c, [\mathrm{Fe/H}]\}\big)$ is a non-zero constant.

So, the probability of the $\mathcal{DM}$ for given star is proportional to the product of the likelihood of $\mathcal{DM}$ and the *prior probability* of $\mathcal{DM}$ (e.g., Eq 2).

$$\mathrm{P}\big(\mathcal{DM} \mid \{m, c, [\mathrm{Fe/H}]\}\big) \propto \mathscr{L}\big(\mathcal{DM}\big)\mathrm{p}_{\mathrm{prior}}\big(\mathcal{DM}\big) \tag{2}$$

The *prior probability* for the DM in Eq. 2 can be incorporated independently, and the main task is to derive $\mathscr{L}\big(\mathcal{DM}\big)$. In deriving $\mathscr{L}\big(\mathcal{DM}\big)$, we must in turn incorporate any *prior* information about other parameters that play a role, such as the giant-branch luminosity function, $\mathrm{p_{prior}}\big(\mathrm{M}\big)$, or the metallicity distribution of halo giants, $\mathrm{p_{prior}}\big([\mathrm{Fe/H}]\big)$. This is done via

$$\mathscr{L}\big(\mathcal{DM}\big) = \int\int \mathrm{p}\big(\{m, c, [\mathrm{Fe/H}]\} \mid \mathcal{DM}, \mathrm{M}, \mathrm{FeH}\big)\mathrm{p_{prior}}\big(\mathrm{M}\big)\mathrm{p_{prior}}\big(\mathrm{FeH}\big)\mathrm{dM\ dFeH}. \quad (3)$$

Here we use FeH to denote the metallicity of the model, while we use [Fe/H] for the observed metallicity of the star.

3.2. Observables and Priors

The direct observables we obtain from SEGUE and SSPP are the extinction corrected apparent magnitudes, colors, metallicities, and their corresponding errors $\big(r_0,\ (g-r)_0,\ [\mathrm{Fe/H}],\ \Delta r_0,$ $\Delta(g-r)_0,\ \Delta[\mathrm{Fe/H}]\big)$. Figure 2 shows that the most common stars are the intrinsically fainter blue giants, as we would expect from the giant-branch luminosity function. Hereafter, we keep using c and m instead of $(g-r)_0$ and r_0 for convenience and generality in the expression of the formulas.

In our analysis, we can and should account for three pieces of prior (external) information or knowledge about the RGB population that go beyond the immediate measurement of the one object at hand: $\mathrm{p_{prior}}(\mathcal{DM})$, $\mathrm{p_{prior}}\big(\mathrm{M}\big)$ and $\mathrm{p_{prior}}\big([\mathrm{Fe/H}]\big)$ (shown as Eq. 1 and Eq. 3).

The *prior probability* of $\mathcal{DM}$ reflects any information on the radial density profile of the Milky Way's stellar halo. Vivas & Zinn (2006) and Bell et al. (2008) indicated that the radial halo stellar density follows a power law $\rho \propto \mathrm{r}^{\alpha}$, with the best value of $\alpha = -3$, and reasonable values of $-2 > \alpha > -4$; this implies $\mathrm{p_{prior}}(\mathcal{DM})\mathrm{d}\mathcal{DM} = \rho 4\pi \mathrm{r}^2\mathrm{dr}$, $\mathrm{p_{prior}}(\mathcal{DM}) \propto \mathrm{e}^{\frac{(3+\alpha)\log_\mathrm{e}10}{5}\mathcal{DM}}$. Quite fortuitously, the *prior probability* for $\mathcal{DM}$ turns out to be flat for the radial stellar density of a power law of $\rho \propto \mathrm{r}^{-3}$. Given that the $\mathscr{L}\big(\mathcal{DM}\big)$ approximatively follows a Gaussian distribution with the mean of $\mathcal{DM}_0$ and the standard deviation of $\Delta\mathcal{DM}$ (here $\Delta\mathcal{DM}$ is the error of $\mathcal{DM}$), the $\mathrm{p_{prior}}(\mathcal{DM})$ will shift the estimate of $\mathcal{DM}_0$ by $\frac{(3+\alpha)\log_\mathrm{e}10}{5}(\Delta\mathcal{DM})^2$, but with basically no change in $\Delta\mathcal{DM}$. Therefore, the shifts in the mean $\mathcal{DM}$ caused by $\mathrm{p_{prior}}(\mathcal{DM})$ can be neglected for values of $-2 > \alpha > -4$ (i.e. $\frac{(3+\alpha)\log_\mathrm{e}10}{5}(\Delta\mathcal{DM})^2 \ll \Delta\mathcal{DM}$).

The *prior probability* of the absolute magnitude M can be inferred from the nearly

universal luminosity function of the giant branch of old stellar populations. Specifically, we derive it from the globular clusters M5 and M30 (Sandquist et al. 1996, 1999), and from the Basti theoretical luminosity function (Pietrinferni et al. 2004). Figure 3 (top panel) shows that the luminosity functions for the RGBs derived from the globular clusters in the different bands are consistent with each other, and also consistent with the Basti theoretic luminosity functions for the metal-rich and metal-poor cases. All the luminosity functions follow linear functions with similar slope, k = 0.32, as a result that the luminosity functions are insensitive to changes in the metallicity and wave bands. According to p(M)dM = p(L)dL and M ~ -2.5logL, the luminosity function p(M) $\propto 10^{\rm kM}$ means p(L) $\propto {\rm L}^{-2.5{\rm k}-1}$. We conclude that the luminosity function for the giant branch follows p(L) $\propto {\rm L}^{-1.8}$, shown as the dashed line in Figure 3.

Our *prior probability* for [Fe/H] results from an empirical approach. In the SEGUE target selection, the K giants were split into four sub-categories: red K giants, l-color K giants, proper motion K giants, and serendipitous K giants. This suggests that one should adopt the overall metallicity distribution of each sub-category as the [Fe/H] prior for any one star in this sub-category (Figure 4). Figure 4 shows the metallicity distribution along with apparent magnitude in the upper panel, and the four [Fe/H] priors in the lower panel. It can be seen that the four sub-categories have different metallicity distributions. For a star that has approximately the mean metallicity, this prior should leave $\mathscr{L}\big(\mathcal{DM}\big)$ unchanged, because the individual metallicity error is smaller than the spread of the $\mathrm{p_{prior}}\big([\mathrm{Fe/H}]\big)$. However, for a star of seemingly very low metallicity, the prior implies that this has been more likely a metallicity-underestimate of a (intrinsically) less metal-poor star, which would mean an overestimated distance modulus.

3.3. Color-Magnitude Fiducials

To obtain distance estimates, we determine an estimate of the absolute magnitude of each star using its $(g-r)_0$ color and a set of giant-branch fiducials for clusters with metallicities ranging from -2.38 to $+0.39$, and then use the star's apparent magnitude (corrected for reddening using the estimates of Schlegel et al. 1998) to obtain its distance. We prefer to use *fiducials*, rather than *model-isochrone* giant branches wherever possible, because isochrone giant branches cannot reproduce cluster fiducials with sufficient accuracy.

We derived such fiducials, using the globular clusters M92, M13, and M71, and the open cluster NGC 6791, which have accurate *ugriz* photometry from the DAOphot reductions of An et al. (2008). For stars brighter than $g \sim 14.5$, the SDSS imager saturates, so we supplemented the giant-branch fiducials for the three globular clusters using the $u'g'r'i'z'$

photometry of Clem et al. (2008). We transformed to *ugriz* using the transformations given in Tucker et al. (2006). We give our adopted values of [Fe/H], reddening, and distance modulus for each cluster in Table 1. In addition, we changed the locus of the M71 fiducial slightly by only using stars which were known members. We supplemented the fiducials with a solar metallicity giant branch from the Basti α-enhanced isochrones (Pietrinferni et al. 2004). Figure 5 shows the four fiducials and one theoretical isochrone. The color at a given M and [Fe/H], $c\big(\mathrm{M}, [\mathrm{Fe/H}]\big)$ can then be interpolated from these color-magnitude fiducials.

Given the sparse sampling of M – $(g-r)_0$ space by the four isochrones, we need to construct interpolated fiducials. We do this by quadratic interpolation of $c\big(\mathrm{M}, [\mathrm{Fe/H}]\big)$, based on the three nearest fiducial points in color, and construct a dense color table for given M and [Fe/H], which will be used for Eq. 4. Extrapolation beyond the metal-poor and metal-rich boundaries and the tip of the RGB would be poorly constrained. Therefore, we use these limiting fiducials instead for the rare cases of stars with [Fe/H] < -2.38 or [Fe/H] $> +0.39$. Table 3 shows an interpolated fiducial with [Fe/H] $= -1.18$; the entire catalog of 20 interpolated fiducials with [Fe/H] ranging from -2.38 to $+0.39$ is provided in the electronic edition of the Journal. While there is more than one way to interpolate the colors, such as quadratic or piecewise linear, we have checked and found that different interpolation schemes lead to an uncertainty less than $\sim \pm 0.02$ mag in color, due to the sparsity of the fiducials.

3.4. Red Giant-Branch Stars vs. Red-Clump Giants

In addition, we have chosen not to assign distances to stars which lie on the giant branch below the level of the horizontal branch (HB). This is because the red horizontal-branch or red-clump (RC) giants in a cluster have the same color as these stars, but quite different absolute magnitude, and the SSPP log g estimate is not sufficiently accurate to discriminate between the two options. We derive a relation between [Fe/H] and the $(g-r)_0$ color of the giant branch at the level of the horizontal branch using eight clusters with *ugriz* photometry from An et al. (2008), with cluster data given in Table 2. The [Fe/H] and $(g-r)_0^{HB}$ for the HB/RC of the clusters follow a quadratic polynomial, $(g-r)_0^{HB} = 0.086[\mathrm{Fe/H}]^2 + 0.38[\mathrm{Fe/H}] + 0.96$, as shown in Figure 2. We then use this polynomial and its [Fe/H] estimate to work out, for each star, whether it is on the giant branch above the level of the HB; it turns out that more than half of the candidate K giants fall into the region of RGB - HB ambiguity.

Ultimately, we are left with 4781 stars that appear to be clearly on the RGB, above the level of the HB, according to the SSPP log g and the Mg index check. Of these, 195 satisfy

the target criteria for red K giants, 463 the criteria for proper motion K giants, and 3231 the l-color K-giant criteria. Another 892 were serendipitous identifications: stars targeted in other categories which nevertheless were giants. Figure 2 shows the distribution of the apparent magnitudes, r_0, and metallicities, [Fe/H], along with the color, $(g-r)_0$.

Besides the contamination from HB/RC stars, we need to consider possible contamination of our sample by asymptotic giant-branch (AGB) stars, because it is not possible for us to distinguish between RGB and AGB stars with our spectra. While the difference in absolute magnitude can be large (varying from ~ 0.8 mag, implying a 40% distance underestimate, at the blue end of our giant color range to a negligible difference at the giant-branch tip), the proportion of our giants which are on the AGB is relatively small. We used both the luminosity function of Sandquist & Bolte (2004) for the globular cluster M5 and evolutionary tracks from Basti isochrones for old populations of metallicity –2.6 and –1.0 to estimate the percentage of stars which are on the AGB. We find that for the most metal-poor stars, around 10% will be AGB stars, while for stars with [Fe/H] close to –1.0 the fraction is near 20%.

3.5. Implementation

For any given star, the observables are its apparent magnitude and associated error, $\big(m_{\rm i}, \Delta m_{\rm i}\big)$, its color and error $\big(c_{\rm i}, \Delta c_{\rm i}\big)$, and its metallicity and error $\big([{\rm Fe/H}]_{\rm i}, \Delta[{\rm Fe/H}]_{\rm i}\big)$. The $\mathcal{DM}$ and the data are linked through the absolute magnitude M via: $m_{\rm i} = {\rm M} + \mathcal{DM}_{\rm i}$ and the fiducial $c\big({\rm M}, {\rm FeH}\big)$, which we presume to be a relation of negligible scatter. Now we can incorporate the errors of the data and the specific priors on the stellar luminosity and metallicity distribution when calculating $\mathscr{L}\big(\mathcal{DM}\big)$ (see Eq. 3).

In practice, the errors on color, apparent magnitude, and metallicity can be approximated as Gaussian functions, in which case $\mathrm{p}\big(\{m, c, [{\rm Fe/H}]\} \mid \mathcal{DM}, {\rm M}, {\rm FeH}\big)$ (see Eq. 3) is modeled as a product of Gaussian distributions with mean and Delta $\big(c_{\rm i}, \Delta c_{\rm i}\big)$, $\big(m_{\rm i}, \Delta m_{\rm i}\big)$, and $\big([{\rm Fe/H}]_{\rm i}, \Delta[{\rm Fe/H}]_{\rm i}\big)$:

$$\mathrm{p}\big(\{m, c, [{\rm Fe/H}]\}_{\rm i} \mid \mathcal{DM}, {\rm M}, {\rm FeH}\big) = \frac{1}{\sqrt{2\pi}\Delta c_{\rm i}} \exp\left(-\frac{(c({\rm M}, {\rm FeH}) - c_{\rm i})^2}{2(\Delta c_{\rm i})^2}\right) \times \frac{1}{\sqrt{2\pi}\Delta m_i} \exp\left(-\frac{(\mathcal{DM} + M - m_i)^2}{2(\Delta m_i)^2}\right) \times \frac{1}{\sqrt{2\pi}\Delta[{\rm Fe/H}]_i} \exp\left(-\frac{(FeH - [{\rm Fe/H}]_i)^2}{2(\Delta[{\rm Fe/H}]_i)^2}\right) \quad (4)$$

For Equation 3, we use the priors $\mathrm{p}_{\rm prior}\big({\rm M}\big)$, based on the luminosity function of the giant

branch, $\mathrm{p}\big(\mathrm{L}\big) \propto \mathrm{L}^{-1.8}$ (Figure 3), and $\mathrm{p_{prior}}\big([\mathrm{Fe/H}]\big)$, based on the metallicity distributions of the K-giant sub-categories (Figure 4).

For any K giant with $\{m_{\rm i}, c_{\rm i}, [\mathrm{Fe/H}]_{\rm i}\}$, we can then calculate $\mathscr{L}\big(\mathcal{DM}\big)$ by computing the integral of a bivariate function (Eq. 3) over dM and dFeH, using iterated Gaussian quadrature. The best estimate and the error in $\mathcal{DM}$ are then estimated using the peak of the likelihood of $\mathcal{DM}$ ($\mathcal{DM}_{\rm peak}$) and its central 68% interval ($\frac{\mathcal{DM}_{84\%}-\mathcal{DM}_{16\%}}{2}$).

To speed up the determination of the integral in Eq. 3, we look up $c\big(\mathrm{M}, [\mathrm{Fe/H}]\big)$ in a pre-calculated, finely sampled color table instead of an actual interpolation. This approach can provide a consistent c for given M and [Fe/H], if the pre-prepared color table is suitable. We use a color table, $c\big(\mathrm{M}, [\mathrm{Fe/H}]\big)$, of size 7000×8000, with $-3.5 < \mathrm{M} < 3.5$ and $-3.58 < [\mathrm{Fe/H}] < +0.56$.

4. Results

4.1. Distances for the SDSS/SEGUE K giants

From §3.4, we obtain the Bayesian estimates of the distance moduli and their uncertainties from the peak of $\mathscr{L}\big(\mathcal{DM}\big)$ and its central 68% interval. At the same time, we obtain estimates for the intrinsic luminosities by $\mathrm{M}_r = r_0 - \mathcal{DM}_{\rm peak}$, distances to the Sun by $\mathrm{d} = 10^{\frac{\mathcal{DM}+5}{5}}$, and Galactocentric distances by taking the Sun at $\mathrm{R}_\odot = 8.0$ kpc. This results in the main entries in our public catalog: the best estimates of the distance moduli and their uncertainties ($\mathcal{DM}_{\rm peak}$, $\Delta\mathcal{DM}$), distance moduli at $(5\%, 16\%, 50\%, 84\%, 95\%)$ confidence of $\mathscr{L}\big(\mathcal{DM}\big)$ ($\mathcal{DM}_{5\%}$,$\mathcal{DM}_{16\%}$,$\mathcal{DM}_{50\%}$,$\mathcal{DM}_{84\%}$, $\mathcal{DM}_{95\%}$), distances to the Sun, and their errors (d, Δd), Galactocentric distances and corresponding errors ($\mathrm{r_{GC}}$, $\Delta \mathrm{r_{GC}}$), and the absolute magnitudes along with the errors (M_r, $\Delta \mathrm{M}_r$) for 4781 K giants. In addition, we also include the sky position (RA, Dec), extinction-corrected apparent magnitudes, r_0, colors, $(g-r)_0$, heliocentric radial velocities, RV, and corresponding errors, as well as the SSPP atmospheric parameters, $\mathrm{T_{eff}}$, [Fe/H], log g, in the catalog for convenient use. Table 4 shows an example of the on-line table of the K giants. The complete version of this table is provided in the electronic edition of the Journal.

Figure 7 illustrates the overall properties of the ensemble of distance estimates. The top two panels show the mean precisions of 12% in Δd/d and ± 0.25 mag in $\mathcal{DM}$; these panels also show that the fractional distances are less precise for more nearby stars, because they tend to be stars on the lower part of the giant branch, which is steep in the color-magnitude diagram, particularly at low metallicities.

The bottom panel of Figure 7 shows that the mean error in M_r is ± 0.25 mag, and that faint giants have less precise intrinsic luminosity estimates. Figure 8 (upper panel) shows the distribution of K giants on the CMD. There are more stars in the lower part of the giant branch, which is consistent with the prediction of the luminosity function. The lower panel of Figure 8 shows that stars in the upper part of the RGB have more precise distances than those in the lower part of the CMD, because the fiducials are much steeper near the sub-giant branch. This is equivalent to the fact that the fractional distance precision is higher for the largest distances (see Figure 7).

The giants in our sample stars lie in the region of $5 - 110$ kpc from the Galactic center and 5 kpc from the disk. There are 1478 stars beyond 30 kpc, 270 stars beyond 50 kpc, and 43 stars beyond 80 kpc (cf. The 5 red giants beyond 50 kpc in Battaglia et al. (2005), 16 halo stars beyond 80 kpc in Deason et al. (2012) and no BHB stars beyond 80 kpc in Xue et al. (2008, 2011)). Our sample comprises the largest sample of distant stellar halo stars with measured radial velocities and distances to date.

4.2. The Impact of Priors

In this section we briefly analyze how important the priors actually were in deriving the distance estimates. For each star, the evaluation of Eq. 3 using Eq. 4 and the interpolated fiducials results in $\mathscr{L}\big(\mathcal{DM}\big)$ (Figure 6), i.e., the likelihood of the distance modulus, *before* folding in an explicit prior on $\mathcal{DM}$, but *after* accounting for the priors on M and [Fe/H] (Eq. 3). In this section we present some example $\mathscr{L}\big(\mathcal{DM}\big)$, but foremost show what the systematic impact on $\mathcal{DM}$ is of neglecting the M and [Fe/H] priors.

When estimating the distance to a given star, without the benefit of external prior information, one would evaluate Eq. 3 presuming that $\mathrm{p_{prior}}\big(\mathrm{M}\big)$ and $\mathrm{p_{prior}}\big([\mathrm{Fe/H}]\big)$ are constant.

To test the impact of $\mathrm{p_{prior}}\big(\mathrm{M}\big)$, we estimate the distances for two cases. No priors applied ($\mathrm{p_{prior}}\big(\mathrm{M}\big) = 1$ and $\mathrm{p_{prior}}\big([\mathrm{Fe/H}]\big) = 1$); and only the prior on the luminosity function applied ($\mathrm{p}\big(\mathrm{L}\big) \propto \mathrm{L}^{-1.8}$ and $\mathrm{p_{prior}}\big([\mathrm{Fe/H}]\big) = 1$). The distance modulus estimate that neglects the explicit priors is denoted as $\mathrm{DM_0}$, while the distance modulus with only $\mathrm{p_{prior}}\big(\mathrm{M}\big)$ applied is marked as $\mathrm{DM_L}$. The top panel of Figure 9 illustrates the importance of including the 'luminosity prior', by showing the systematic difference in $\mathcal{DM}$ that results from neglecting it. For stars near the tip of the giant branch the bias is very small, but for stars near the bottom of the giant branch, the mean systematic bias of neglecting the prior information is 0.08 mag, with systematic bias of ~ 0.2 mag in some cases.

To test the impact of $\mathrm{p_{prior}}\big([\mathrm{Fe/H}]\big)$, we estimate the distances where only the metallicity prior was applied, and mark the relevant $\mathcal{DM}$ as $\mathrm{DM_{[Fe/H]}}$. Compared with the distance modulus with no priors applied, $\mathrm{DM_0}$, we find $\mathrm{p_{prior}}\big([\mathrm{Fe/H}]\big)$ can correct a mean overestimate of 0.03 mag on the $\mathcal{DM}$ for the metal-poor stars and a mean underestimate of 0.02 mag on the $\mathcal{DM}$ for the metal-rich ones, but the neglect of the metallicity prior causes a smaller bias in $\mathcal{DM}$ than neglecting the luminosity prior (0.05 *vs*. 0.2 mag at maximum), as shown in Figure 9 (middle panel). The distance modulus bias caused by neglecting both priors is presented in the bottom panel of Figure 9. Neglecting both priors causes a mean bias of 0.08 mag and a maximum bias of 0.2 mag in distance modulus.

4.3. Distance Precision Test using Clusters

We use known members from three clusters (M92, M13 and NGC6791) to test the estimates of the $\mathcal{DM}$, because they have more spectroscopic member giants than M71. Figure 10 shows all the member stars in each cluster and the member giants used for the test are highlighted. The Bayesian method was applied to estimate $\mathcal{DM}$ for each member giant, adopting the same luminosity prior, but a Gaussian distribution of [Fe/H] centered at the literature cluster metallicity, and with the same [Fe/H] dispersion as known cluster members, as the metallicity prior. Figure 11 shows our estimates of $\mathcal{DM}$ are consistent with the literature $\mathcal{DM}_{\mathrm{GC}}$ (shown in Table 1), derived by main-sequence fitting, to within 1 σ.

5. Summary and Conclusions

We have implemented a probabilistic approach to estimate the distances for SEGUE K giants in the Galactic halo. This approach folds all available observational information into the calculation, and incorporates external information through priors, resulting in a $\mathcal{DM}$ likelihood for each star that provides both a distance estimate and its uncertainty.

The priors adopted in this work are the giant-branch luminosity function derived from globular clusters, and the ensemble metallicity distributions for different SEGUE K-giant target categories. We show that these priors are needed to prevent systematic overestimate of the distance moduli by up to 0.2 mag. The role of the priors are important, and make the results more reasonable.

We use empirical color-magnitude fiducials from old stellar clusters to obtain the predicted colors $c\big(\mathrm{M}, [\mathrm{Fe/H}]\big)$, which are needed to calculate $\mathscr{L}\big(\mathcal{DM}\big)$. Ultimately, the best estimates of the distance moduli and their errors can be estimated using the peak and central

68% interval of $\mathscr{L}(\mathcal{DM})$.

With this approach we obtain Bayesian estimates of distance moduli, and thus, absolute magnitudes and distances, for 4781 K giants that have a mean distance precision of 12%, or ± 0.25 mag in $\mathcal{DM}$ and M_r. The sample contains 270 stars beyond $r_{GC} = 50$ kpc, which makes it by far the largest sample of distant stellar halo stars with measured radial velocities and distances to date.

We present an online catalog containing the distance moduli, observed information and SSPP atmospheric parameters for the 4781 SEGUE K giants. For each object in the catalog we also list some of the basic observables such as (RA,Dec), extinction-corrected apparent magnitudes and colors, as well as the information obtained from the spectra– heliocentric radial velocities plus SSPP atmospheric parameters. In addition, we provide the Bayesian estimates of the distance moduli, distances to the Sun, Galactocentric distances, the absolute magnitudes and their uncertainties, along with the distance moduli at $(5\%, 16\%, 50\%, 84\%, 95\%)$ confidence of $\mathscr{L}(\mathcal{DM})$.

We tested the accuracy of our distance estimates using giants in the old clusters M13, M92 and NGC6791, which have SEGUE observations. We found that the distance estimates for the individual cluster member stars derived with our approach are consistent with the literature distance moduli of the clusters.

We caution the reader that the n(d, [Fe/H]) cannot be used to obtain the halo profile and the metallicity distribution directly, because the complex SEGUE selection function needs to be taken into account.

Funding for SDSS-III has been provided by the Alfred P. Sloan Foundation, the Participating Institutions, the National Science Foundation, and the U.S. Department of Energy Office of Science. The SDSS-III web site is http://www.sdss3.org/.

SDSS-III is managed by the Astrophysical Research Consortium for the Participating Institutions of the SDSS-III Collaboration including the University of Arizona, the Brazilian Participation Group, Brookhaven National Laboratory, University of Cambridge, Carnegie Mellon University, University of Florida, the French Participation Group, the German Participation Group, Harvard University, the Instituto de Astrofisica de Canarias, the Michigan State/Notre Dame/JINA Participation Group, Johns Hopkins University, Lawrence Berkeley National Laboratory, Max Planck Institute for Astrophysics, Max Planck Institute for Extraterrestrial Physics, New Mexico State University, New York University, Ohio State University, Pennsylvania State University, University of Portsmouth, Princeton University, the Spanish Participation Group, University of Tokyo, University of Utah, Vanderbilt University,

University of Virginia, University of Washington, and Yale University.

This work was made possible by the support of the Max-Planck-Institute for Astronomy, and supported by the National Natural Science Foundation of China under grant Nos. Y111181001, 11233004 and 11003017, and supported by the Young Researcher Grant of National Astronomical Observatories, Chinese Academy of Sciences. This paper was partially supported by the DFG's SFB-881 grant 'The Milky Way System'.

H. Morrison acknowledges funding of this work from NSF grant AST-0098435.

YSL and TCB acknowledge partial support of this work from grants PHY 02-16783 and PHY 08-22648: Physics Frontier Center / Joint Institute for Nuclear Astrophysics (JINA), awarded by the U.S. National Science Foundation.

HRJ acknowledges support from the National Science Foundation under award number AST-0901919.

JJ acknowledges NSF's grants AST-0807997 and AST-0707948.

SL reasearch is partially supported by the INAF PRIN grant "Multiple populations in Globular Clusters: their role in the Galaxy assembly".

REFERENCES

Allende Prieto, C., Sivarani, T., Beers, T. C., et al. 2008, AJ, 136, 2070

An, D., Johnson, J. A., Clem, J. L., et al. 2008, ApJS, 179, 326

Battaglia, G. 2007, PhD thesis, Kapteyn Astronomical Institute, University of Groningen

Battaglia, G., Helmi, A., Morrison, H., et al. 2005, MNRAS, 364, 433

Bell, E. F., Zucker, D. B., Belokurov, V., et al. 2008, ApJ, 680, 295

Bond, H. E. 1980, ApJS, 44, 517

Brogaard, K., Bruntt, H., Grundahl, F., et al. 2011, A&A, 525, A2

Burnett, B. & Binney, J. 2010, MNRAS, 407, 339

Burnett, B., Binney, J., Sharma, S., et al. 2011, A&A, 532, A113

Carraro, G., Villanova, S., Demarque, P., et al. 2006, ApJ, 643, 1151

Carretta, E., Gratton, R. G., Clementini, G., & Fusi Pecci, F. 2000, ApJ, 533, 215

Clem, J. L., Vanden Berg, D. A., & Stetson, P. B. 2008, AJ, 135, 682

Deason, A. J., Belokurov, V., Evans, N. W., et al. 2012, ArXiv e-prints

Eisenstein, D. J., Weinberg, D. H., Agol, E., et al. 2011, AJ, 142, 72

Fukugita, M., Ichikawa, T., Gunn, J. E., et al. 1996, AJ, 111, 1748

Gratton, R., Bragaglia, A., Carretta, E., & Tosi, M. 2006, ApJ, 642, 462

Grundahl, F., Stetson, P. B., & Andersen, M. I. 2002, A&A, 395, 481

Gunn, J. E., Carr, M., Rockosi, C., et al. 1998, AJ, 116, 3040

Gunn, J. E., Siegmund, W. A., Mannery, E. J., et al. 2006, AJ, 131, 2332

Kraft, R. P. & Ivans, I. I. 2003, PASP, 115, 143

Lee, Y. S., Beers, T. C., Sivarani, T., et al. 2008a, AJ, 136, 2022

Lee, Y. S., Beers, T. C., Sivarani, T., et al. 2008b, AJ, 136, 2050

Lenz, D. D., Newberg, J., Rosner, R., Richards, G. T., & Stoughton, C. 1998, ApJS, 119, 121

Morrison, H. L., Flynn, C., & Freeman, K. C. 1990, AJ, 100, 1191

Morrison, H. L., Mateo, M., Olszewski, E. W., et al. 2000, AJ, 119, 2254

Morrison, H. L., Norris, J., Mateo, M., et al. 2003, AJ, 125, 2502

Perryman, M. A. C., Lindegren, L., Kovalevsky, J., et al. 1997, A&A, 323, L49

Peterson, R. C. & Green, E. M. 1998, ApJ, 502, L39

Pier, J. R., Munn, J. A., Hindsley, R. B., et al. 2003, AJ, 125, 1559

Pietrinferni, A., Cassisi, S., Salaris, M., & Castelli, F. 2004, ApJ, 612, 168

Ratnatunga, K. U. & Bahcall, J. N. 1985, ApJS, 59, 63

Sandquist, E. L. & Bolte, M. 2004, ApJ, 611, 323

Sandquist, E. L., Bolte, M., Langer, G. E., Hesser, J. E., & Mendes de Oliveira, C. 1999, ApJ, 518, 262

Sandquist, E. L., Bolte, M., Stetson, P. B., & Hesser, J. E. 1996, ApJ, 470, 910

Schlegel, D. J., Finkbeiner, D. P., & Davis, M. 1998, ApJ, 500, 525

Smolinski, J. P., Lee, Y. S., Beers, T. C., et al. 2011, AJ, 141, 89

Starkenburg, E., Helmi, A., Morrison, H. L., et al. 2009, ApJ, 698, 567

Stoughton, C., Lupton, R. H., Bernardi, M., et al. 2002, AJ, 123, 485

Tucker, D. L., Kent, S., Richmond, M. W., et al. 2006, Astronomische Nachrichten, 327, 821

Vivas, A. K. & Zinn, R. 2006, AJ, 132, 714

Xue, X.-X., Rix, H.-W., Yanny, B., et al. 2011, ApJ, 738, 79

Xue, X. X., Rix, H. W., Zhao, G., et al. 2008, ApJ, 684, 1143 [X08]

Yanny, B., Rockosi, C., Newberg, H. J., et al. 2009, AJ, 137, 4377

York, D. G., Adelman, J., Anderson, Jr., J. E., et al. 2000, AJ, 120, 1579

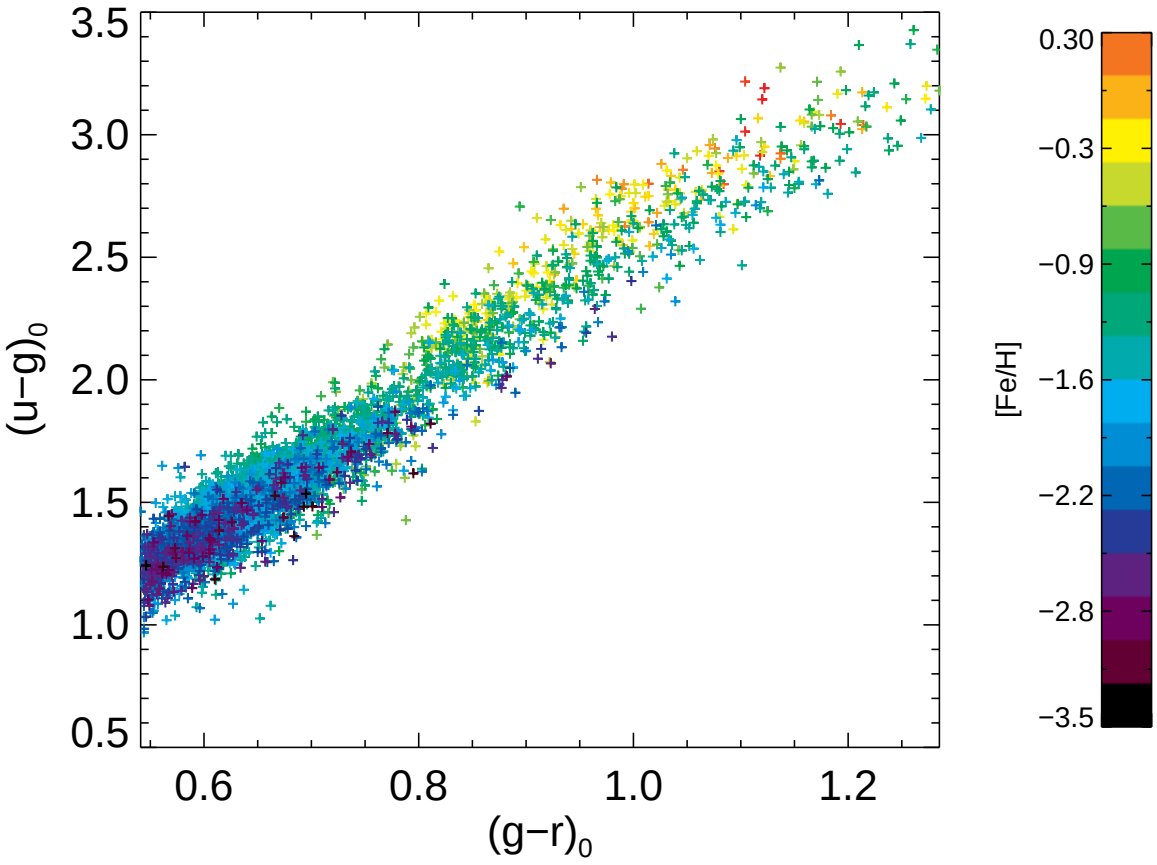

Fig. 1.—: Color-color diagram for confirmed K giants in our sample, with DR9 SPP estimates for [Fe/H] color coded as shown in the vertical bar.

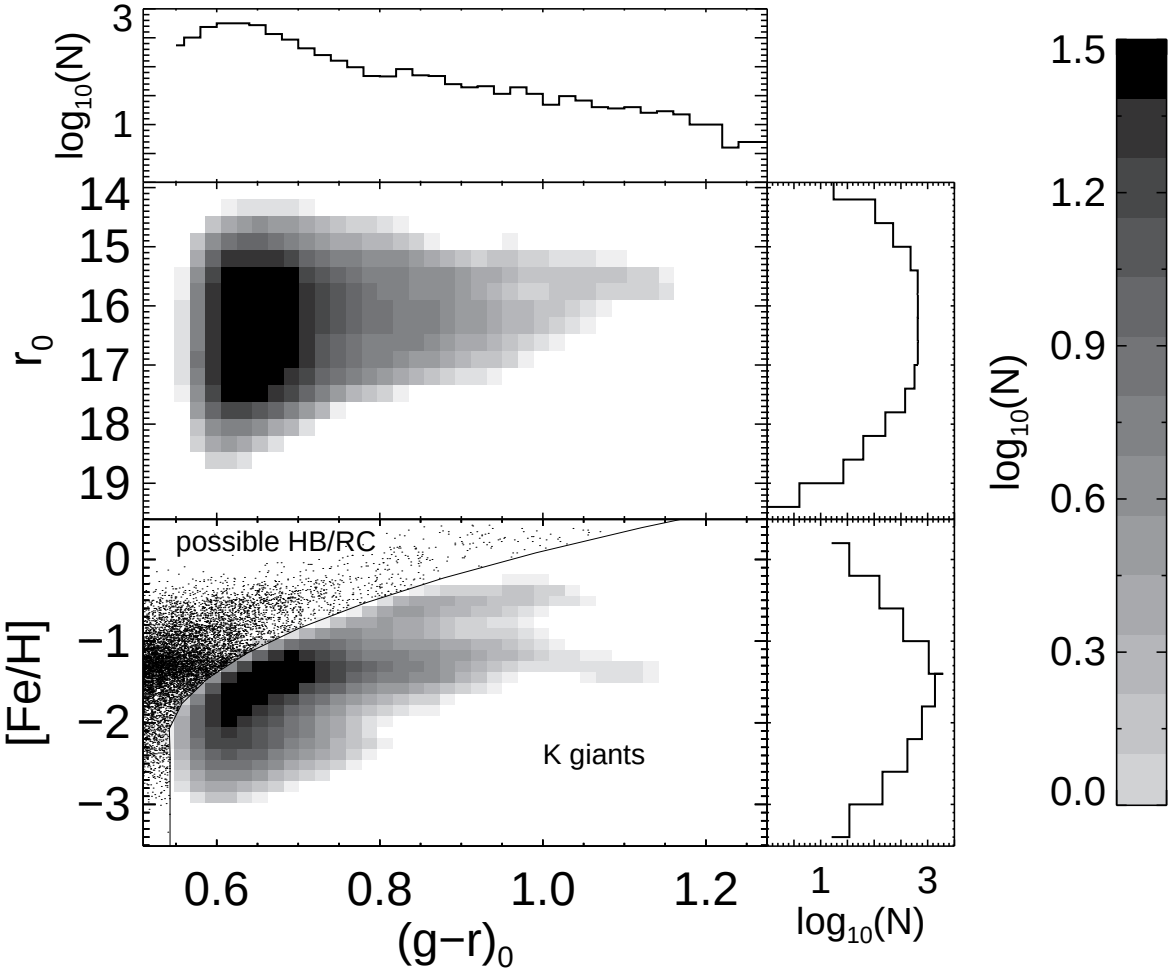

Fig. 2.—: Distribution of our K-giant sample in the color-magnitude and color-metallicity plane. It can be seen that the most common stars are the intrinsically fainter blue giants, as we would expect from the giant-branch luminosity function. The possible HB/RC stars are over-plotted as black dots, and the relation between [Fe/H] and $(g-r)_0^{HB}$ is marked as the black solid line.

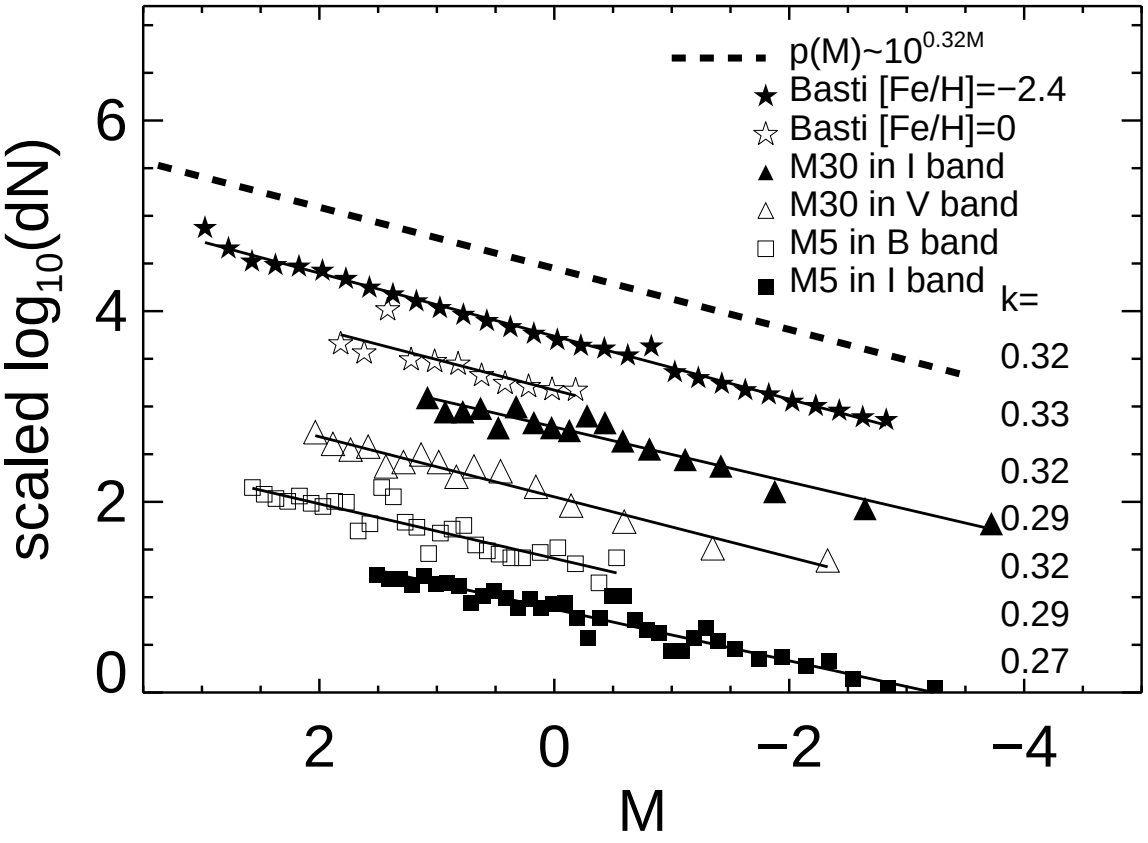

Fig. 3.—: Luminosity functions for the giant branch of two globular clusters in different bands, compared with two theoretical giant-branch luminosity functions. We scaled $\log_{10}(\mathrm{dN})$ to make the luminosity functions separate from each other, because the slope is the important parameter to test whether the luminosity functions are consistent. All the luminosity functions follow power laws with nearly the same slope of 0.32, so that the theoretical and observational luminosity functions are consistent, and both are insensitive to changes in metallicity and passbands. Therefore, the prior probability adopted for the absolute magnitude in the analysis is $\mathrm{p(M)} = 10^{0.32\mathrm{M}}/17.788$, which is based on a variety of theoretical and empirical giant-branch luminosity functions, and whose integral over [–3.5,+3.5] has been normalized to unity. 'k' stands for the slope.

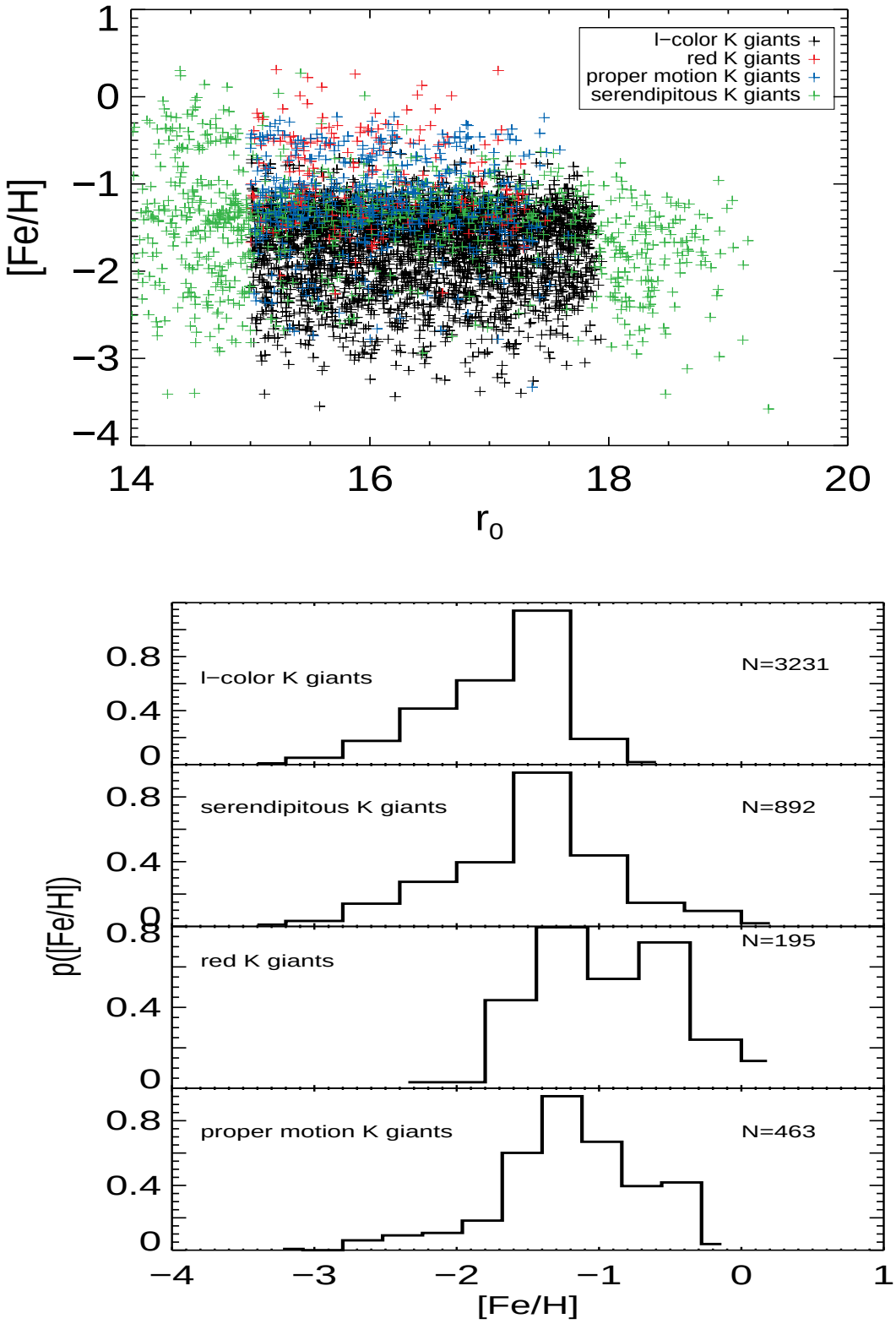

Fig. 4.—: (Upper panel) Variation of the metallicity distribution with apparent r_0 magnitude for four sub-categories. (Lower panel) The four [Fe/H] priors adopted in this work. The integral of p([Fe/H]) has been normalized to unity.

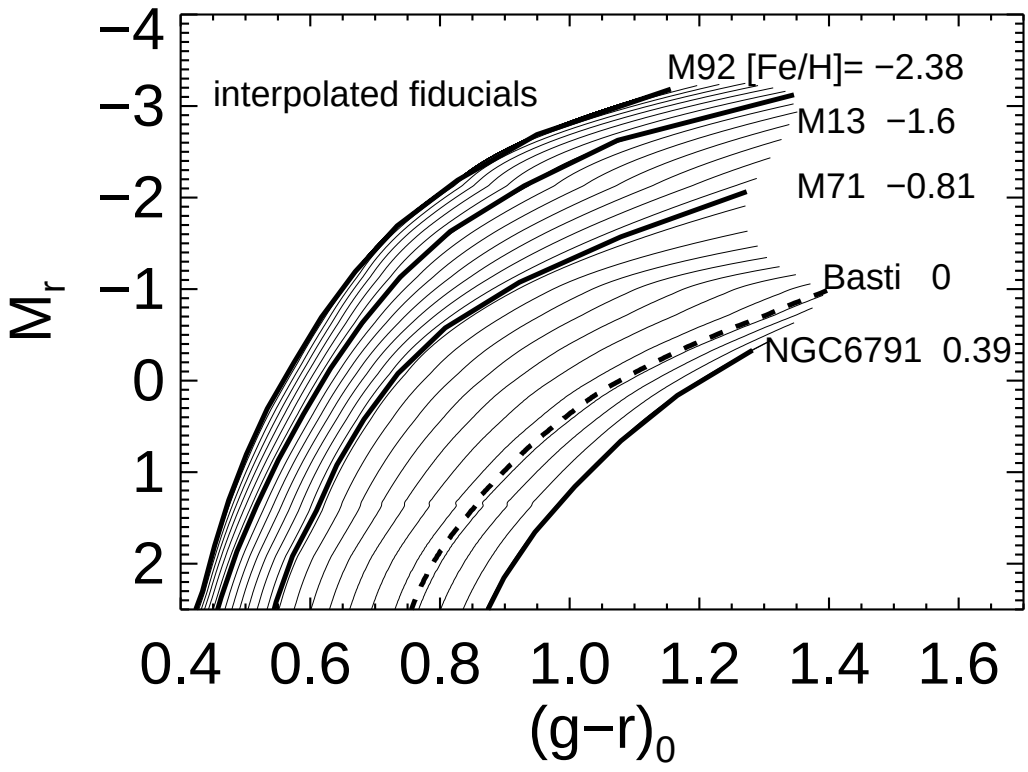

Fig. 5.—: Interpolation of the four giant-branch fiducials (thick lines), to obtain the relation, $(g-r)_0 = f(M_r, \mathrm{[Fe/H]})$, for any set of ($\mathrm{M}_r$, [Fe/H]). The thin lines show a set of interpolated fiducials. No values outside the extreme fiducials are used.

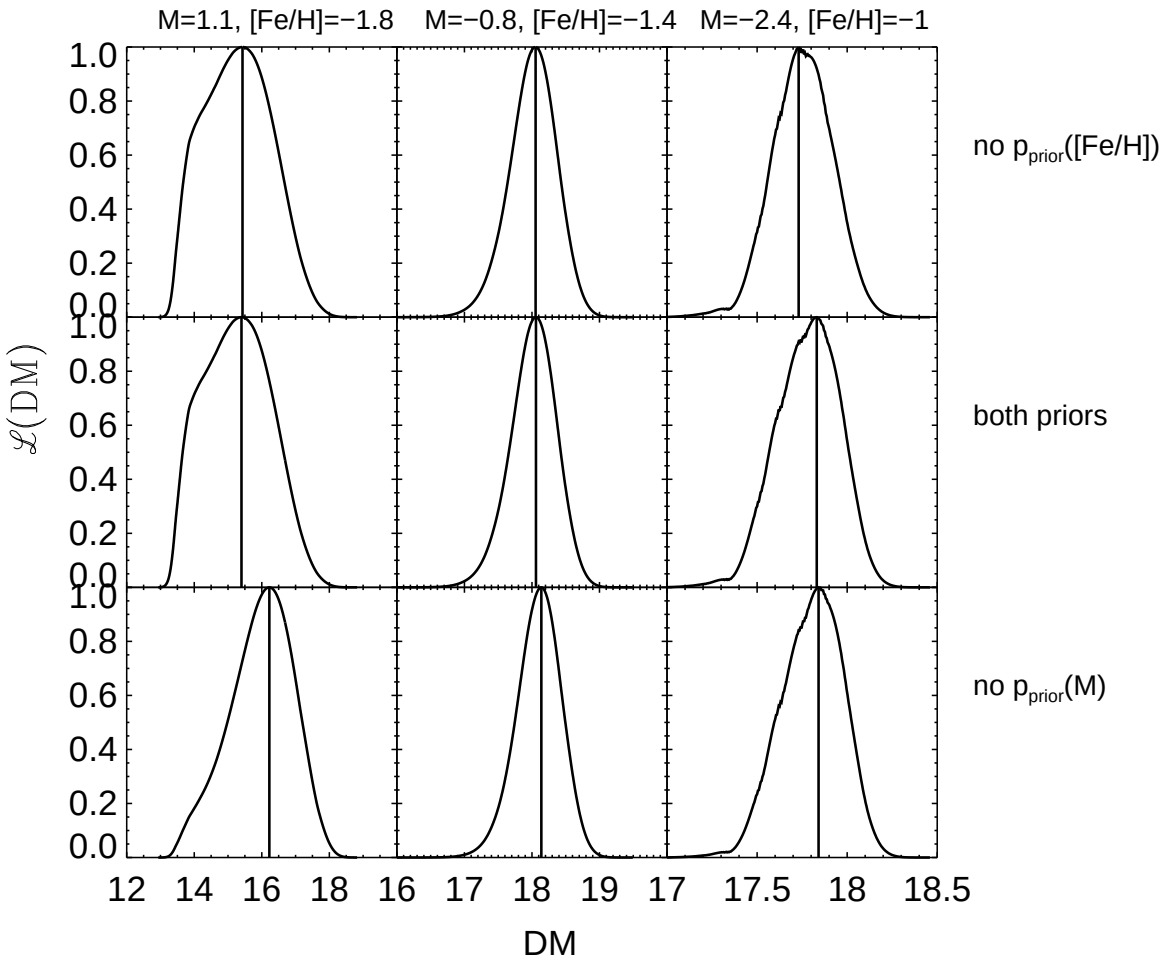

Fig. 6.—: Examples of $\mathscr{L}(\mathcal{DM})$ for three stars, with and without accounting for the metallicity and luminosity-function priors (see §4.2). The black line indicates the most likely $\mathcal{DM}$ under the three assumptions, showing the systematic overestimate of the $\mathcal{DM}$ if priors are neglected.

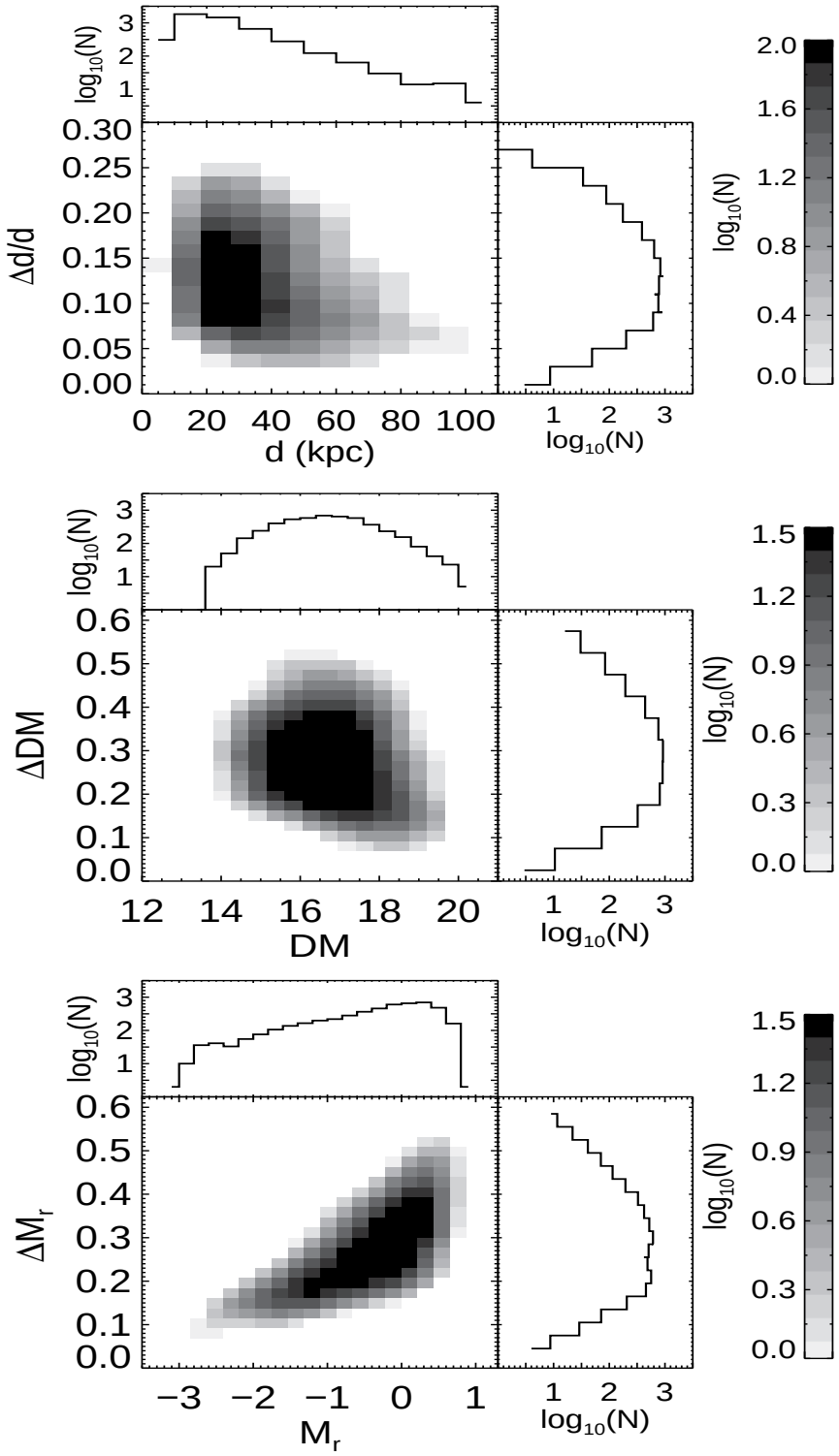

Fig. 7.—: Results of the distance estimates for 4781 K giants. (Upper panel) The distribution of the relative error in distance *vs.* distance. (Middle panel) The distribution of the error in absolute magnitude *vs.* absolute magnitude. (Lower panel) The distribution of the error in distance moduli *vs.* distance moduli. Note that the fractional distance estimates are less precise for nearby stars, because the lower part of the giant branch (less luminous, therefore more nearby) is steep in the color-magnitude diagram, particularly at low metallicities (see Figure 5).

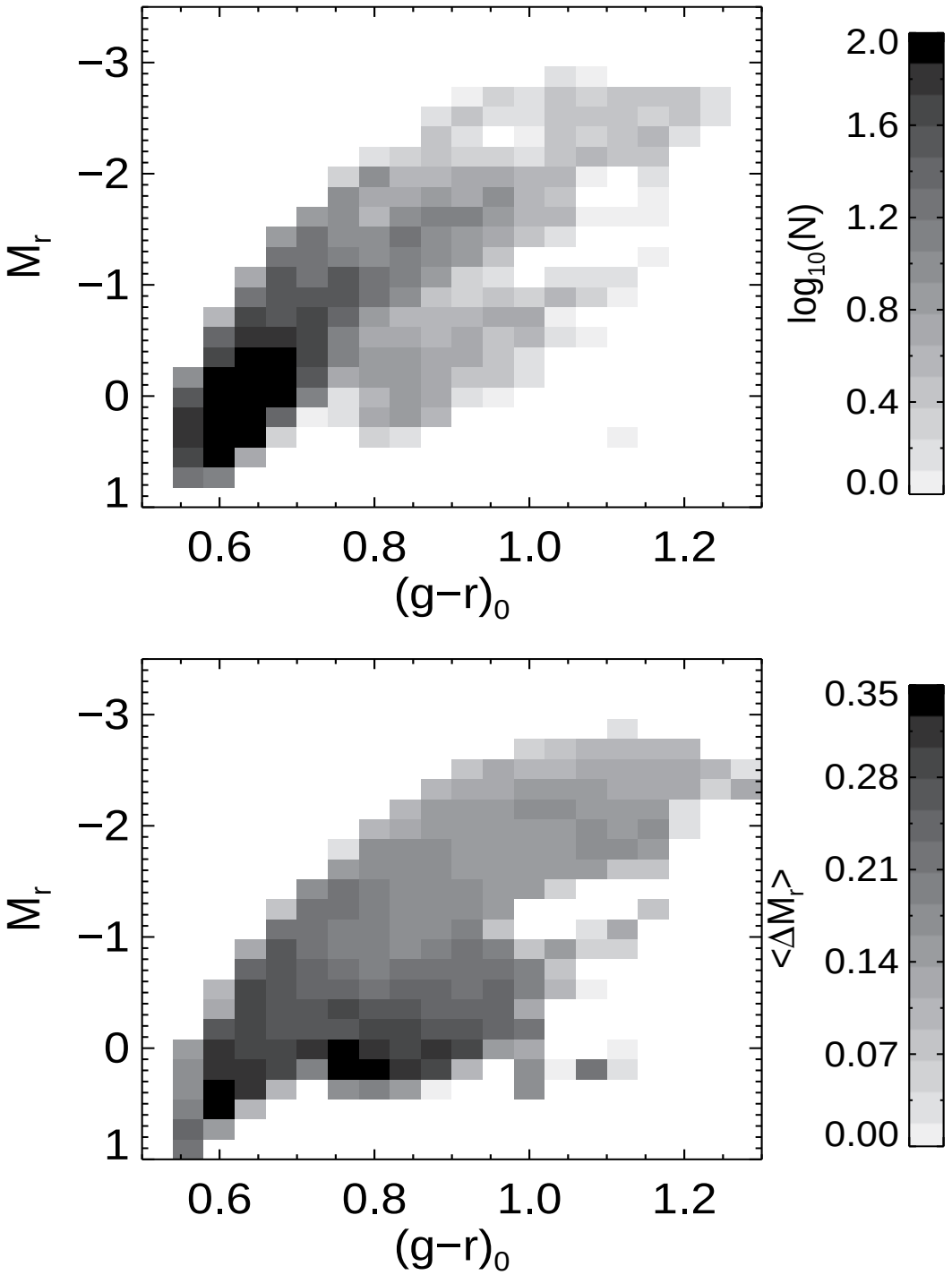

Fig. 8.—: (Upper panel) The distribution of K giants on the CMD plot. (Lower panel) The distribution of the mean error in the absolute magnitude, M_r, as a function of M_r and $(g-r)_0$. The upper panel shows that the sample contains a large fraction of relatively nearby giants of moderate luminosity ($M_r \sim 0$). (Lower panel) The luminosity estimates for stars in lower part of the CMD are less precise, because the isochrones are much steeper in this part, especially for low metallicities.

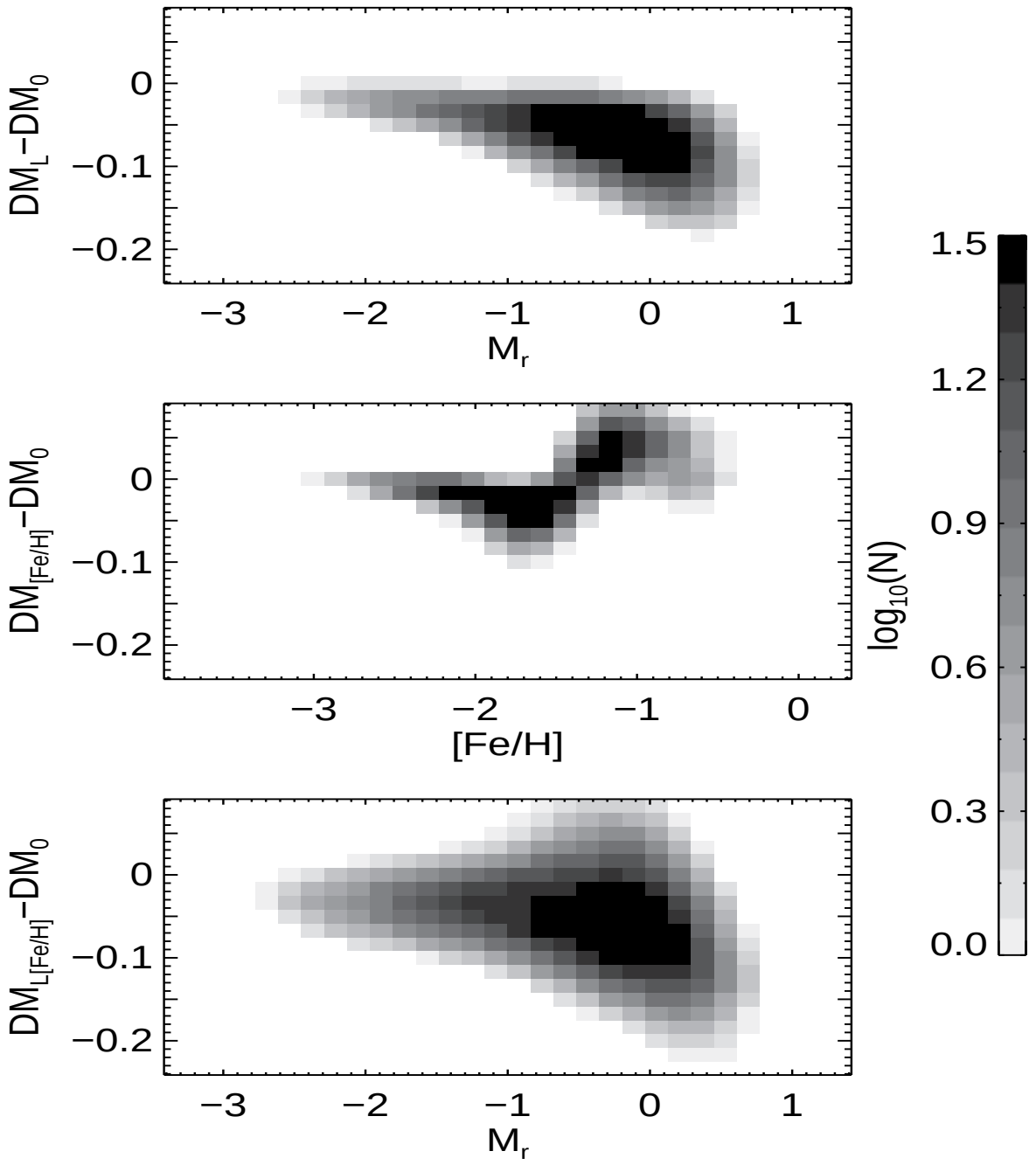

Fig. 9.—: The distance modulus bias caused by neglecting the priors on the luminosity function and metallicity distribution of the K giants. The luminosity function prior can help correct a mean overestimate of 0.1 mag in the distance moduli, and a maximum overestimate of ~ 0.2 mag in some cases. While the [Fe/H] prior's impact is much smaller, it can help correct a mean of 0.02 mag overestimate or underestimate on the distances in the metal-poor or metal-rich tails. The bottom panel shows the total impacts of the luminosity prior and the metallicity prior.

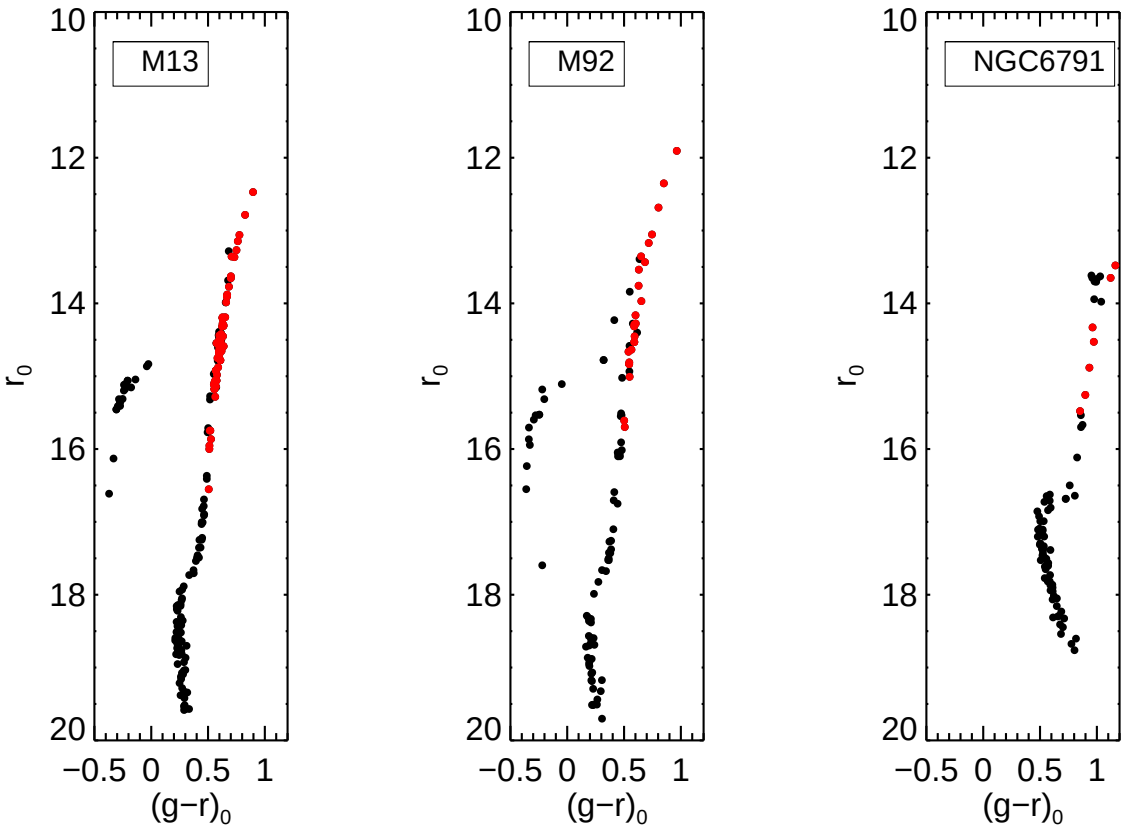

Fig. 10.—: The color-magnitude diagrams for the three clusters used for distance precision test. The black dots are cluster member stars that we used to derive the fiducials, and the red dots are the K giants we used to examine the Bayesian approach.

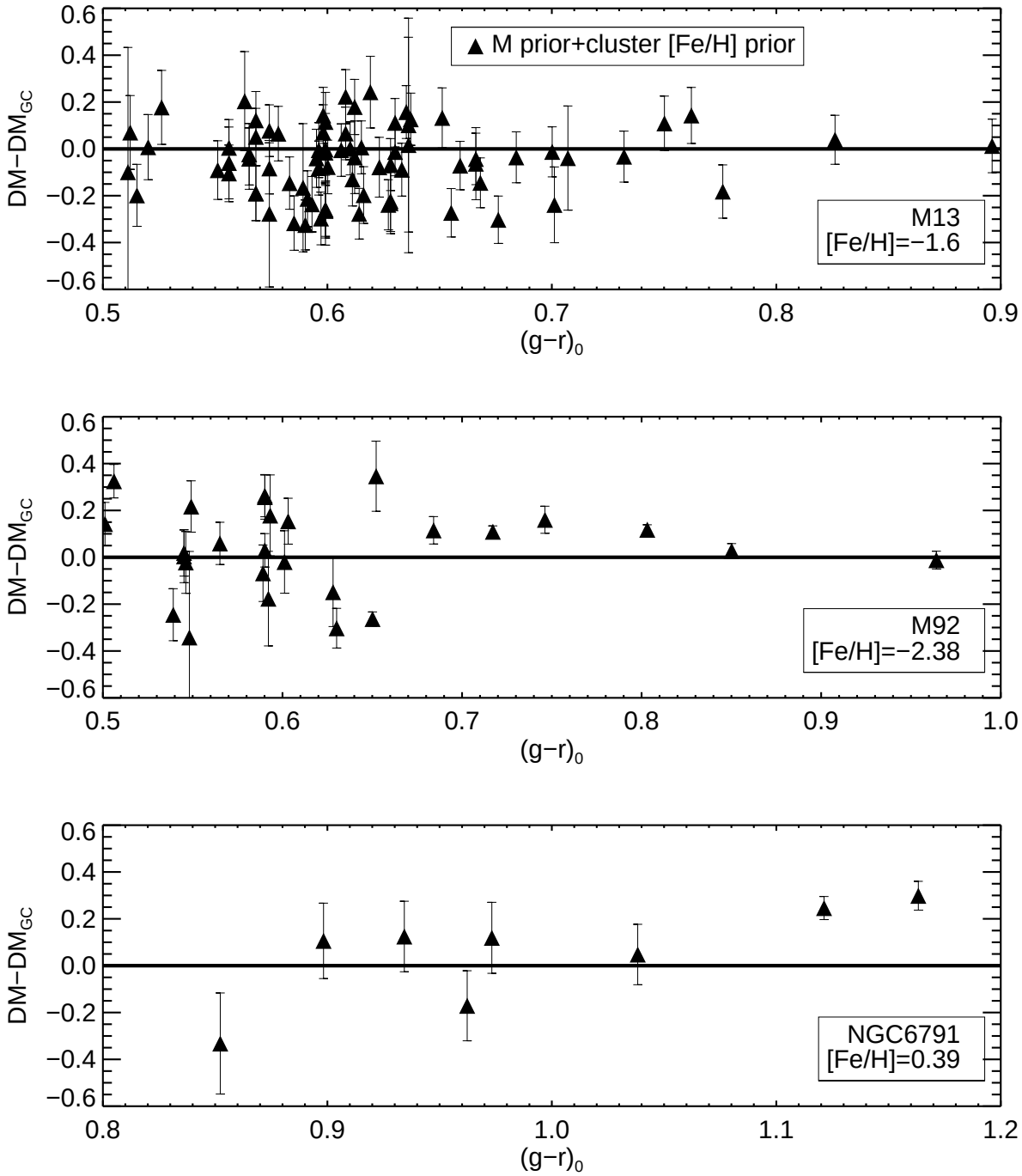

Fig. 11.—: The difference between our estimate of the Clusters' $\mathcal{DM}$ and the literature $\mathcal{DM}$ *vs.* $(g-r)_0$. Black triangles indicate the case using the cluster metallicity priors, which indicates that the Bayesian estimates of $\mathcal{DM}$ are consistent with the literature $\mathcal{DM}_{\rm GC}$, to within 1 σ.

Table 1:: Parameters of the Fiducial Clusters

NGC	Messier	E(B-V)	$(m-M)_0$	[Fe/H]
6341	M92	0.02[a]	14.64[b]	–2.38[a]
6205	M13	0.02[a]	14.38[b]	–1.60[a]
6838	M71	0.28[c]	12.86[c]	–0.81[a]
6791		0.16[d]	13.01[d]	+0.39[e]

[a]Kraft & Ivans (2003); their globular cluster metallicity scale is based on the FeII lines from high-resolution spectra of giants.

[b]Carretta et al. (2000); $(m-M)_0$ derived from the Hipparcos sub-dwarf fitting.

[c]Grundahl et al. (2002); $(m-M)_0$ derived from the Hipparcos (Perryman et al. 1997) sub-dwarf fitting.

[d]Brogaard et al. (2011); $(m-M)_0$ is based on $(m-M)_v$ assuming $A_v = 3.1E(B-V)$.

[e]simple average of the [Fe/H] +0.29, +0.47, +0.4 and +0.39 by Brogaard et al. (2011), Gratton et al. (2006), Peterson & Green (1998), and Carraro et al. (2006) respectively.

Table 2:: Metallicity and Color of the Red Horizontal-Branch Onset for the Eight Clusters in An et al. (2008)

Name of Clusters	[Fe/H]	$(g-r)_0^{HB}$
NGC6791	+0.39	1.13
M5	–1.26	0.61
M3	–1.50	0.59
M13	–1.60	0.58
M53	–1.99	0.54
M92	–2.38	0.53
M15	–2.42	0.53

The first column are the names of the clusters and the next two columns contains the [Fe/H] of the clusters and the extinction corrected color $(g-r)_0$.

Table 3:: Interpolated Fiducial at [Fe/H]=–1.18

$(g-r)_0$	M_r	[Fe/H]
0.47	3.00	–1.18
0.52	2.01	–1.18
0.57	1.31	–1.18
0.61	0.68	–1.18
0.66	0.14	–1.18
0.70	–0.30	–1.18
0.75	–0.65	–1.18
0.79	–0.94	–1.18
0.84	–1.18	–1.18
0.88	–1.39	–1.18
0.93	–1.58	–1.18
0.98	–1.75	–1.18
1.02	–1.90	–1.18
1.07	–2.04	–1.18
1.11	–2.19	–1.18
1.16	–2.33	–1.18
1.20	–2.45	–1.18
1.25	–2.55	–1.18
1.29	–2.65	–1.18
1.34	–2.74	–1.18

This is an example of one interpolated fiducial with [Fe/H]=–1.18. The entire catalog of 20 interpolated fiducials with [Fe/H] ranging from –2.38 to +0.39 is provided in the electronic edition of the Journal.

Table 4:: List of 4781 K Giants Selected from SDSS DR9

RA(J2000) (deg)	Dec(J2000) (deg)	r_0 (mag)	Δr_0 (mag)	$(g-r)_0$ (mag)	$\Delta(g-r)_0$ (mag)	RV (kms^{-1})	ΔRV (kms^{-1})	T_{eff} (K)	[Fe/H]	log g	$\mathcal{DM}_{peak}$ (mag)	$\mathcal{DM}_{5\%}$ (mag)
359.5853	36.4018	15.139	0.010	0.713	0.022	–71.9	2.1	4979	–2.17	1.80	16.59	16.15
358.5352	36.2383	16.762	0.010	0.623	0.014	–198.4	3.5	5140	–1.32	2.40	16.42	16.08
358.2261	36.1001	16.002	0.020	0.923	0.028	–60.4	4.5	4496	–2.78	1.10	18.59	18.39
357.3861	35.7609	16.239	0.010	0.647	0.022	–172.6	3.1	5062	–1.48	2.00	16.33	15.84
357.7179	37.0025	15.519	0.010	0.685	0.014	–63.4	2.3	4936	–2.10	1.50	16.71	16.33

RA(J2000) (deg)	Dec(J2000) (deg)	$\mathcal{DM}_{16\%}$ (mag)	$\mathcal{DM}_{50\%}$ (mag)	$\mathcal{DM}_{84\%}$ (mag)	$\mathcal{DM}_{95\%}$ (mag)	$\Delta\mathcal{DM}$ (mag)	M_r (mag)	ΔM_r (mag)	d (kpc)	Δd (kpc)	r_{GC} (kpc)	Δr_{GC} (kpc)
359.5853	36.4018	16.32	16.54	16.73	16.84	0.21	–1.45	0.21	20.79	1.94	24.59	1.84
358.5352	36.2383	16.21	16.41	16.61	16.73	0.20	0.34	0.20	19.22	1.75	23.01	1.65
358.2261	36.1001	18.47	18.58	18.68	18.73	0.10	–2.59	0.10	52.35	2.41	55.34	2.39
357.3861	35.7609	16.03	16.31	16.57	16.73	0.27	–0.09	0.27	18.48	2.25	22.20	2.11
357.7179	37.0025	16.48	16.68	16.84	16.94	0.18	–1.19	0.18	22.01	1.80	25.62	1.72

The first two columns contains the position (RA, Dec) for each object. The magnitude,color, and their errors are in the next four columns: corrected for extinction. The $\mathcal{DM}$ at the peak and $(5\%, 16\%, 50\%, 84\%, 95\%)$ confidence of $\mathscr{L}(\mathcal{DM})$ are listed in the next six columns. $\mathcal{DM}_{peak}$ is the best estimate of the distance modulus for the K giant. The $\Delta_{\mathcal{DM}}$ is the uncertainty of the distance modulus, which is calculated from $(\mathcal{DM}_{84\%} - \mathcal{DM}_{16\%})/2$. The last six columns are absolute magnitude and distances calculated from $\mathcal{DM}_{peak}$, assuming $R_\odot = 8.0$ kpc (i.e. $M_r = r_0 - \mathcal{DM}_{peak}$, $d = 10^{\frac{\mathcal{DM}+5}{5}}$). The complete version of this table is provided in the electronic edition of the Journal. The printed edition contains only a sample.